processes

MDPI

Article

Removal of Primamycin La from Milk Sample Using $ZnCl_2$-Activated Biochar Prepared from Bean Plant as Adsorbent: Kinetic and Equilibrium Calculations

Muradiye Şahin [1,2,*], Yasin Arslan [2], Carlos Roberto Luna-Domínguez [3], Jorge Humberto Luna-Domínguez [3,*] and Ronaldo Câmara Cozza [4,*]

[1] Department of Chemistry, Kırşehir Ahi Evran University, 40100 Kırşehir, Turkey
[2] Department of Nanoscience and Nanotechnology, Faculty of Arts and Science, Burdur Mehmet Akif Ersoy University, 15100 Burdur, Turkey; yasinarslan@mehmetakif.edu.tr
[3] Facultad de Odontología, Universidad Autónoma de Tamaulipas, Tampico 88740, Mexico; carlosrlunad10@gmail.com
[4] Department of Mechanical Manufacturing, Faculty of Technology of Mauá, CEETEPS—State Center for Technological Education "Paula Souza", Mauá 09390-120, Brazil
* Correspondence: muradiye.sahin@ahievran.edu.tr (M.Ş.); jhluna@docentes.uat.edu.mx (J.H.L.-D.); ronaldo.cozza@fatec.sp.gov.br (R.C.C.)

Abstract: In this study, porous biochar (PvBC) was obtained by the pyrolysis of bean (*phaseolus vulgaris*) plant at 600 °C, and then activated biochar (PvBCZn) was synthesized by $ZnCl_2$ activation at an equal biomass ratio (1.0:1.0). Some analytical techniques (SEM-EDX (scanning electron microscopy–energy dispersive X-ray spectroscopy), TGA/DTA (Thermogravimetric/Differential Thermal Analysis), BET (Brunauer–Emmett–Teller), FTIR (Fourier Transform Infrared Spectroscopy) and XRD (X-ray diffraction)) were used to characterize both PvBC and PvBCZn. In addition, their antibiotic sensitivity, water solubility, moisture content and swelling behavior were investigated in detail. Furthermore, both PvBC and PvBCZn were used for the adsorption of primamycin la, an anti-inflammatory drug used in veterinary medicine whose active ingredient is oxytetracycline, in a milk sample. The effect of both pH and adsorbent dosage on the adsorption capacity was investigated. Based on adsorption studies, while the maximum adsorption capacity (q_{max}) of PvBCZn was found to be 188.48 mg/g, that of PvBC was found to be 122.49 mg/g. According to these results, PvBCZn is an excellent adsorbent for the removal of primamycin la from milk samples. The Langmuir isotherm model and the pseudo-second-order kinetic model were more suitable to describe the adsorption behavior of primamycin la. The PvBCZn adsorbent exhibited rapid removal exceeding 75% in the first 20 min and reached equilibrium after about 50 min. In addition, studies on the desorption and reusability of PvBCZn were carried out under the same optimum experimental conditions. The q_{max} value of PvBCZn was found to be 171.40 mg/g even in the fifth cycle, confirming the idea that it is a potential adsorbent for the removal of primamycin la. At the same time, the antimicrobial activity of PvBCZn against *Escherichia coli* bacteria increases its potential to be used in both purification systems and hygiene products.

Keywords: adsorption; bean (*Phaseolus vulgaris*); antibiotic sensitivity; natural biochar; swelling behavior

Academic Editor: Federica Raganati

Received: 22 December 2024
Revised: 8 January 2025
Accepted: 13 January 2025
Published: 15 January 2025

Citation: Şahin, M.; Arslan, Y.; Luna-Domínguez, C.R.; Luna-Domínguez, J.H.; Cozza, R.C. Removal of Primamycin La from Milk Sample Using $ZnCl_2$-Activated Biochar Prepared from Bean Plant as Adsorbent: Kinetic and Equilibrium Calculations. *Processes* **2025**, *13*, 230. https://doi.org/10.3390/pr13010230

1. Introduction

Some milk and dairy products, which are of irreplaceable nutritional importance, may contain undesirable residues, such as veterinary drugs, pesticides, mycotoxins, heavy

metals, dioxins and chemical substance residues [1]. Many of the antibiotics in pollutants remain in active form because they cannot be metabolized in the body [2,3]. Antibiotics belonging to the tetracycline class are effective antibacterial agents with widespread use in the prevention of both human and animal diseases [4]. Oxytetracyclines are the most widely used antibiotics in the tetracycline class for the treatment of various infections in both animals and humans.

Primamycin la is a broad-spectrum antibacterial drug used in horses, goats, cattle and sheep, and its active ingredient, oxytetracycline, can cause harmful and toxic effects on humans even at low concentrations [5]. Milk obtained from lactating cattle, goats and sheep should not be offered for human consumption during treatment and for 12 days (24 milkings) after the last drug application. Not selling milk for 12 days economically harms the producer, while milk sold without waiting for this period harms the consumer. Therefore, the removal of oxytetracycline from both milk and dairy products is very important for both economic and health reasons. The tolerance levels of oxytetracycline in milk have been set by both the United States Food and Drug Administration and the European Union as 300 μg kg^{-1} and 100 μg kg^{-1}, respectively [6].

Currently, many different methods, such as photocatalytic degradation [7,8], biological treatment [9,10], electrochemical treatment [11,12], filtration [13,14], ultrasound degradation [15,16], advanced oxidative process [17,18] and adsorption [19–22], are used to remove antibiotics. With respect to other methods, adsorption has widely been used in the removal of tetracycline class antibiotics in recent years due to its environmental friendliness, high adsorption capacity, low cost, high efficiency, ease of application and short processing time [23,24]. The use of biomass as an adsorbent for the removal of pharmaceuticals is currently a popular research topic. Biochar (BC), a solid carbonaceous product of biomass pyrolysis, has advantages, such as economic viability, carbon sequestration potential, a porous structure, various surface functional groups and a large surface area [25,26]. For these reasons, activated carbon and biochar, which are porous carbonaceous materials, have attracted attention as adsorbents for the removal of both organic and inorganic pollutants in recent years [27–31]. The activation of biochar after the pyrolysis process is generally used to further strengthen biochar porosity, charge density and surface area [32]. There are many chemical activating agents, such as KOH, NaOH, NH_3, K_2CO_3 and $ZnCl_2$, which are alkaline, and HNO_3, H_3PO_4 and H_2SO_4, which are acidic and used for activation. Among them, $ZnCl_2$ has been widely used as both an activator and co-pyrolysis agent for the synthesis of BC [32,33].

In this study, the remaining branches, leaves, husks and stalks of beans after harvesting from gardens, fields and along roadsides were used to produce BC to add value and eliminate these wastes. Then, the biochar was activated with $ZnCl_2$, and both porous biochar (PvBC) and activated biochar (PvBCZn) were used for the removal of primamycin la from a milk sample. Kinetic and isotherm studies of the best adsorbent were carried out. In general, one of the biggest problems in terms of human health is the increase in the number of microorganisms resistant to antibiotics. The uncontrolled application of antibiotics to lactating animals is one of the most important reasons for the development of resistance. As a result, the treatment of human diseases is delayed, and allergic reactions, such as asthma, etc., are increased in humans, the number of resistant microorganisms in the environment increases, and the quality of important animal products, such as milk, is impaired, causing economic losses [34]. For this reason, antibiotic sensitivity studies were also conducted. Antimicrobial activity studies were performed by the disk diffusion method using erythromycin (10 μg) and chloramphenicol (10 μg) antibiotics for *Staphylococcus aureus* ATCC 25923 and *Escherichia coli* ATCC 35150 bacteria, respectively.

The aim of this study is to determine the potential of converting bean plant, which is an agricultural waste, into both PvBC and PvBCZn and to investigate their uses as

adsorbents in the removal of primamycin la, which is widely used in veterinary medicine, from milk samples. The comparison of adsorption capacities, moisture contents, water solubility, swelling behavior and antimicrobial susceptibility tests of both the obtained PvBC and PvBCZn also provides insights, helping to address the scarcity of drug removal studies using raw milk samples.

2. Materials and Methods

2.1. Chemicals and Reagents

Bean (*Phaseolus vulgaris*) plant residues were collected from agricultural fields in Isparta city in Turkey, and then they were dried and ground with a blender. Zinc chloride hexahydrate ($ZnCl_2 \cdot 6H_2O$) was obtained from Merck, New Jersey/USA. Ultrapure water was used for the preparation of all solutions. Milk sample was obtained from a local vendor and kept in the refrigerator.

2.1.1. Preparation of PvBC and PvBCZn Biochars

Ground bean plant powder, weighing 100 g, was placed in crucibles and burned in a muffle furnace Ankara/Turkey at 600 °C for 30 min. After cooling, it was washed with plenty of ultrapure water (18 MΩ·cm) and dried in an oven at 80 °C. The obtained PvBC was stored in glass bottles. To synthesize activated biochar, both PvBC and $ZnCl_2 \cdot 6H_2O$ were mixed at a weight ratio of 1.0:1.5, and the mixture was stirred in a magnetic stirrer Schwerte/Germany at 500 rpm until homogeneous. Then, the mixture was placed in crucibles and pyrolyzed at 600 °C for 30 min. After cooling, the mixture was washed three times with ultrapure water and filtered. The filtrate was dried in an oven at 80 °C.

2.1.2. Characterization of Biochar and Activated Biochar

SEM-EDX (Carl Zeiss EVO-LS 10), XRD (Bruker D8 Advance, Kα radiation with about 2θ: 10–90°), FTIR (Perkin Elmer Fronter), TG/DTA (SEIKO SII, 7200) and N_2 Adsorption–Desorption Isotherms (Quantachrome Quadrasorb SI, 77K, P/P0~0.99) were used to determine the different surface morphologies, carry out a surface elemental analysis and determine the thermal stability and chemical structures of the prepared biochars. A few drops of NaOH and HCl were used for pH change and measured with a pH meter (Thermo Scientific, Orion 3 Star, Istanbul/Turkey). XRD, FTIR and TG/DTA analyses were performed at Burdur Mehmet Akif Ersoy University/Turkey (Central Laboratuary) and SEM-EDX and N_2 Adsorption–Desorption Isotherms were performed at Çanakakale 18 Mart University/Turkey (Science and Technology Application and Research Centers).

2.2. Adsorption Experiments

A milk sample of 500 mL was heated to 40 °C and then taken into ten falcon tubes and centrifuged at 7000 rpm for 10 min. Then, the filtrate was again heated to 40 °C, centrifuged at 7000 rpm for 10 min and filtered again. The same procedures were repeated once more. A 1000 mL stock solution was prepared by taking 100 mL from the milk sample, and it was centrifuged and filtered three times.

The adsorption of primamycin la using both PvBC and PvBCZn adsorbents was performed with the batch adsorption method. The effects of some experimental parameters, such as pH (3–11) and adsorbent amount (10–50 mg), on the adsorption capacity were investigated. Both adsorption isotherm and kinetic studies were carried out at initial concentrations between 2 and 250 mg/L primamycin la at 298 K for 75 min. The removal/adsorption experiments of primamycin la were performed by using UV-Vis spectrometer (Shimadzu UV-1800, from 200 nm to 1100 nm) at 276 nm.

2.3. Moisture Content, Water Solubility, and Swelling Behavior

The water solubility (*WS*), swelling behavior (*SB*), and moisture content (*MC*) of both PvBC and PvBCZn were determined gravimetrically. Both PvBC and PvBCZn were first weighed (m_0) after being kept in a desiccator. They were then dried at 105 °C for 24 h and weighed again (m_1). Subsequently, the dried PvBC and PvBCZn were immersed in 50 mL of ultrapure water at 25 °C in a shaking water bath for 24 h. After filtration to remove surface water, both PvBC and PvBCZn were weighed again (m_2) and then dried at 105 °C for 24 h. Afterward, they were weighed again (m_3). Furthermore, the water solubility (*WS*), swelling behavior (*SB*) and moisture content (*MC*) were calculated using Equations (1)–(3), respectively [35]:

$$WS(\%) = \left(\frac{m_1 - m_3}{m_1}\right)100\% \quad (1)$$

$$SB(\%) = \left(\frac{m_2 - m_1}{m_1}\right)100\% \quad (2)$$

$$MC(\%) = \left(\frac{m_0 - m_1}{m_0}\right)100\% \quad (3)$$

2.4. Antimicrobial Activity

For antibacterial tests, Gram-positive *Staphylococcus aureus* (Catalog No: ATCC 25923) and Gram-negative *Escherichia coli* (Catalog No: ATCC 35150) were used to evaluate the antibacterial properties of both PvBC and PvBCZn prepared through the disk diffusion method. Freshly activated bacterial cultures on 4 mm thick Mueller Hinton Agar were inoculated onto the entire surface with 0.5 MacFarland setting (in 0.9% NaCl). An amount of 10 µg of erythromycin and 10 µg of chloramphenicol antibiotics were used against both *Staphylococcus aureus* ATCC 25923 and *Escherichia coli* ATCC 35150 bacteria, respectively. The commercial disks impregnated with antibiotics were used for the disk diffusion method. The antibiotic solutions placed in the wells were kept for 30 min, and then the prepared plates were incubated in an oven at 37 °C for between 16 and 18 h.

3. Results and Discussion

3.1. FTIR Spectra and X-Ray Diffraction of Both PvBC and PvBCZn

In the FTIR spectrum of PvBC (Figure 1a), some peaks at about 1450 cm^{-1} (C=C aromatic rings) and 1024 cm^{-1} (C–O groups) [36,37] were observed. Moreover, in the FTIR spectrum of PvBCZn, these peaks were shifted, and a new peak at around 605 cm^{-1} confirmed the presence of metal oxides (Zn–O group) in this material [38].

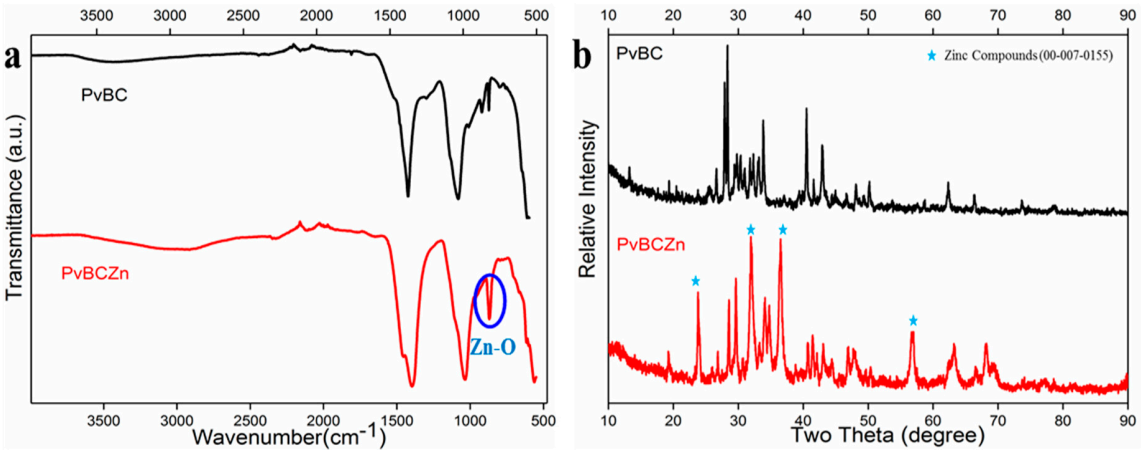

Figure 1. Comparative results of (**a**) FTIR and (**b**) XRD analyses of both PvBC and PvBCZn.

As seen from the XRD of PvBCZn (Figure 1b), the presence of zinc in the structure was confirmed by the observation of JCPDS Card 00-007-0155. In the pyrolysis that took place at 600 °C and accompanied by H_2 gas, Zn^{+2} turned into ZnO. A possible reaction during the pyrolysis step is as follows [22]:

$$5ZnCl_2 \cdot 6H_2O_{(k)} + 26H_{2(g)} \overset{600^{\circ}C}{\underset{\triangle}{\rightarrow}} Zn_5(OH)_8Cl_2 \cdot H_2O_{(k)} + 21H_2O_{(g)} + 4Cl_{2(g)}$$

when FTIR and XRD analyses are evaluated together, it is seen that $ZnCl_2$ activation causes significant changes in the BC structure. The FTIR results confirm the presence of Zn-O bonds, while the XRD analysis supports the formation of the crystal structure of ZnO.

3.2. Nitrogen Gas Adsorption/Desorption Isotherm of Both PvBC and PvBCZn

The nitrogen adsorption/desorption isotherms and the pore size distribution of both PvBC and PvBCZn are shown in Figure 2a,b, respectively. Their isotherms can be considered as Type IV and hysteresis Type H4. It is seen that the S_{BET} (BET-specific surface area) of PvBCZn increases and the V_{total} (total pore volume) decreases. The reason for this is that Zn also settles in the pores apart from its different interactions. The BET-specific surface areas of both PvBC and PvBCZn were found to be 92.3 m^2/g and 101.5 m^2/g, respectively.

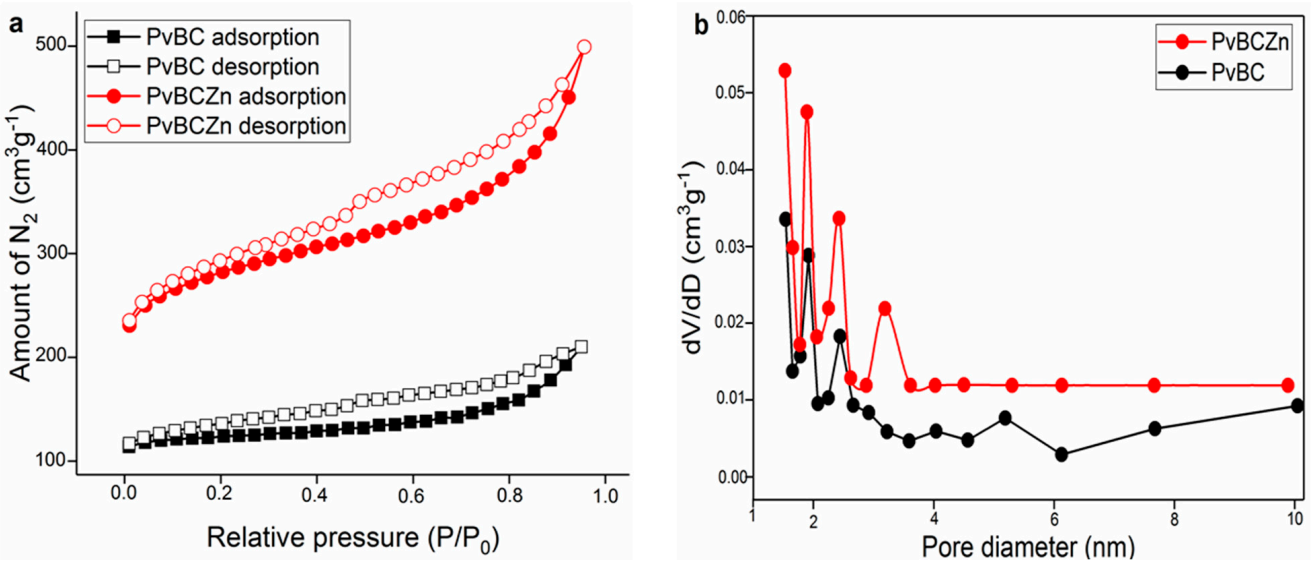

Figure 2. PvBC and PvBCZn: (**a**) nitrogen adsorption/desorption isotherm at 77.3 K and (**b**) pore size distribution.

3.3. Scanning Electron Microscopy–Energy Dispersive X-Ray Spectrometry

The SEM-EDX analysis (Figure 3) also confirmed the activation of PvBC by $ZnCl_2$. The SEM image of PvBCZn (Figure 3b) shows that Zn is deposited in the pores of the biochar surface. In the EDX analysis of PvBCZn, it can be seen that while the amount of C decreased, the presence of Zn was observed, which is in good agreement with the FTIR and XRD results (Figure 1).

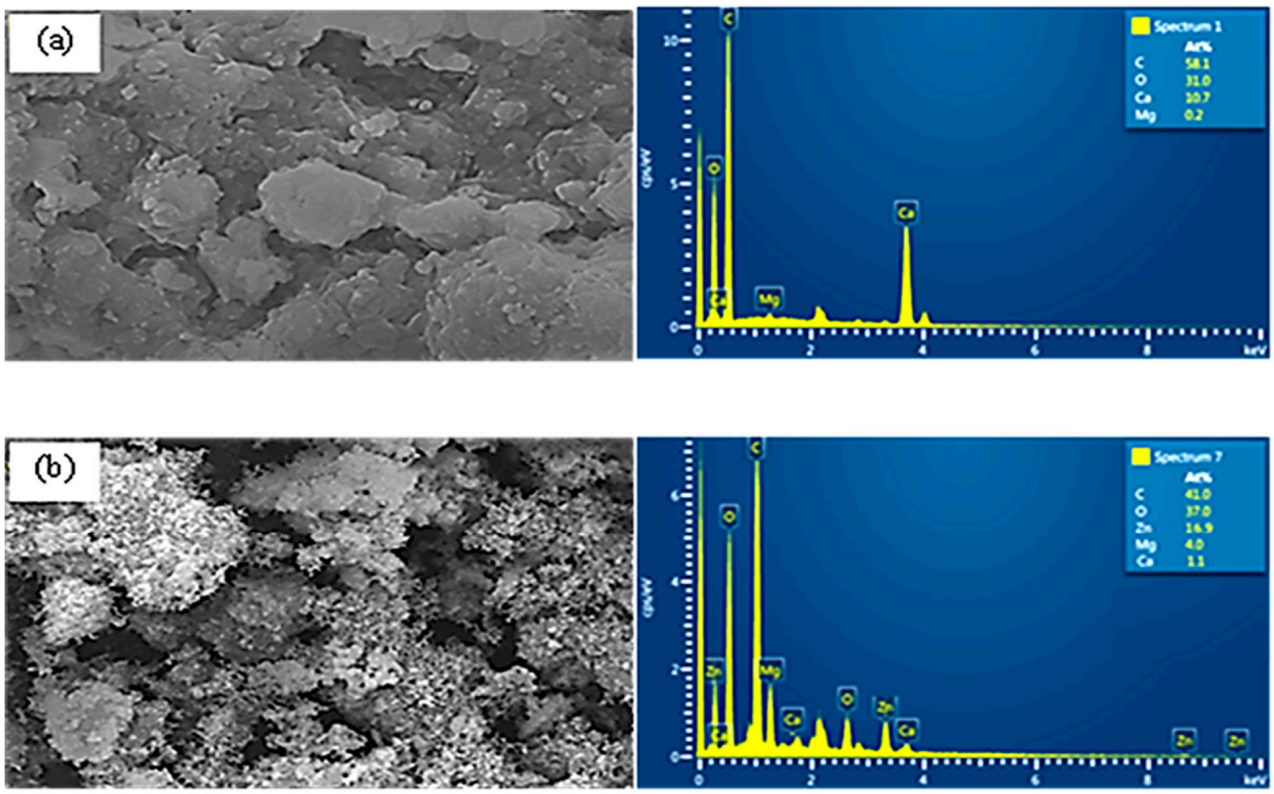

Figure 3. SEM images and EDX analysis of (**a**) PvBC and (**b**) PvBCZn.

The SEM image (Figure 3a) shows that the surface of PvBC has a relatively smooth and dense structure. On the other hand, PvBCZn exhibits a more porous and heterogeneous structure in the SEM image (Figure 3b). The irregularity and increase in voids on the surface indicate that the activation process changes the physical properties of the BC. The EDX analysis reveals that BC contains the main elements: C (58.1%), O (31.0%), Ca (10.7%) and low levels of Mg (0.2%). This result indicates that the BC is carbon based, and the low amount of Mg indicates that the mineral content is limited. The EDX analysis performed after $ZnCl_2$ activation shows that the C (42.0%) and O (37.0%) ratios are reduced, but a significant amount of Zn (16.9%) is observed. The presence of Zn confirms that the activation process was successful, and Zn was incorporated into the BC structure. As a result, $ZnCl_2$ activation significantly changed the surface morphology and elemental composition of BC. The more porous structure and increased Zn content resulting from activation can increase both the adsorption capacity and chemical stability of PvBCZn. These changes can improve the performance of BC, especially in water resistance, ion exchange capacity, and other environmental applications.

3.4. Thermal Analysis of Both PvBC and PvBCZn

Figure 4 shows the thermal profile of both BCs. The thermal behavior was studied for 1 h at a temperature increase of 10 °C per min using an N_2 atmosphere ranging from room temperature to 650 °C. Amounts of 7150 mg of PvBC and 8729 mg of PvBCZn samples were studied, and the mass losses calculated from the TG curves in Figure 4 were found to be 9.79% and 11.45%, respectively. It is seen that this mass loss occurs in four stages: 0–100 °C, 100–250 °C, 250–500 °C and 500–650 °C.

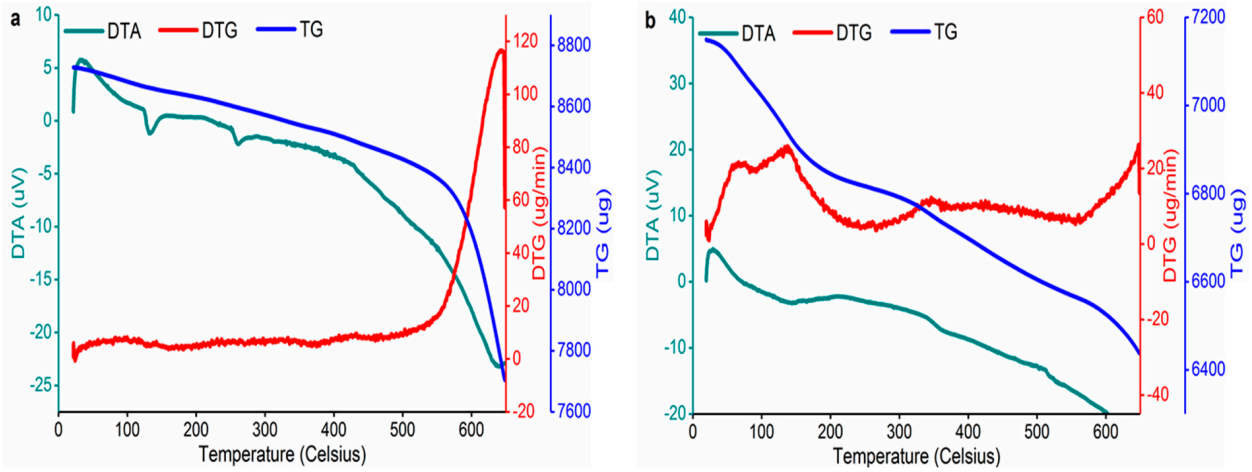

Figure 4. DTA, DTG and TG curves of (**a**) PvBCZn and (**b**) PvBC.

From the endothermic peak seen in the first stage of the DTA curves, it is understood that the reason for the mass loss at this stage is the loss of moisture in the samples. The exothermic peaks seen in the DTA curves (Figure 4a) between the 100–250 °C region and 250–500 °C region are related to chemical reaction or crystallization, which is in agreement with the crystalline phases seen in XRD (Figure 1b). The mass loss in the last stage is the smallest and corresponds to the thermal degradation of the carbon matrix.

3.5. Moisture Content, Water Solubility and Swelling Behavior of Both PvBC and PvBCZn

The water solubility, swelling behavior and moisture content of both PvBC and PvBCZn are given in Table 1, confirming their water resistance.

Table 1. Moisture content—*MC* (%); swelling behavior—*SB* (%); and water solubility—*WS* (%) of both PvBC and PvBCZn.

Sample	Moisture Content—*MC*	Swelling Behavior—*SB*	Water Solubility—*WS*
PvBC	15.14%	12.13%	38.27%
PvBCZn	13.41%	10.58%	35.62%

Table 1 demonstrates that the incorporation of Zn in PvBCZn leads to a reduction in moisture content, water solubility and swelling behavior (water absorption) compared to PvBC. This reduction in moisture content can be attributed to the filling effect of Zn, which occupies the voids within the composite structure, thereby enhancing its resistance to water. Likewise, the possible reason for the decrease in the working behavior values may be the decrease in the voids in the BC matrix. It is thought that the decrease in water solubility of PvBCZn may be caused by the pairing of Zn with the functional group of BC.

3.6. Antimicrobial Activity Results

The disk diffusion results of both PvBC and PvBCZn are given in Table 2. According to antimicrobial activity, while PvBC did not show antimicrobial activity against the Gram-positive bacteria, it showed a smaller inhibition zone diameter against Gram-negative bacteria with respect to PvBCZn. This feature makes both PvBC and PvBCZn usable in water treatment systems and hygiene products.

Table 2. Antimicrobial activities of both PvBC and PvBCZn.

Bacteria	Sample	Inhibition Zone Diameter [mm]
Staphylococcus aureus ATCC 25923	PvBC	0.00
	PvBCZn	9.00
Escherichia coli ATCC 35150	PvBC	17.25
	PvBCZn	23.50

3.7. Adsorption Studies of Primamycin La

Adsorption studies were carried out by taking 50 mL of the stock milk sample whose preparation was described in the "Adsorption Experiments" Section. In the adsorption experiments of Primamycin la with both PvBC and PvBCZn, the effect of some experimental parameters, such as pH (3–11) and adsorbent dosage (10–50 mg), on adsorption was investigated under the conditions of 20 ppm of a 50 mL solution at a 75 min contact time, at room temperature and at a 250 rpm stirring speed (Figure 5).

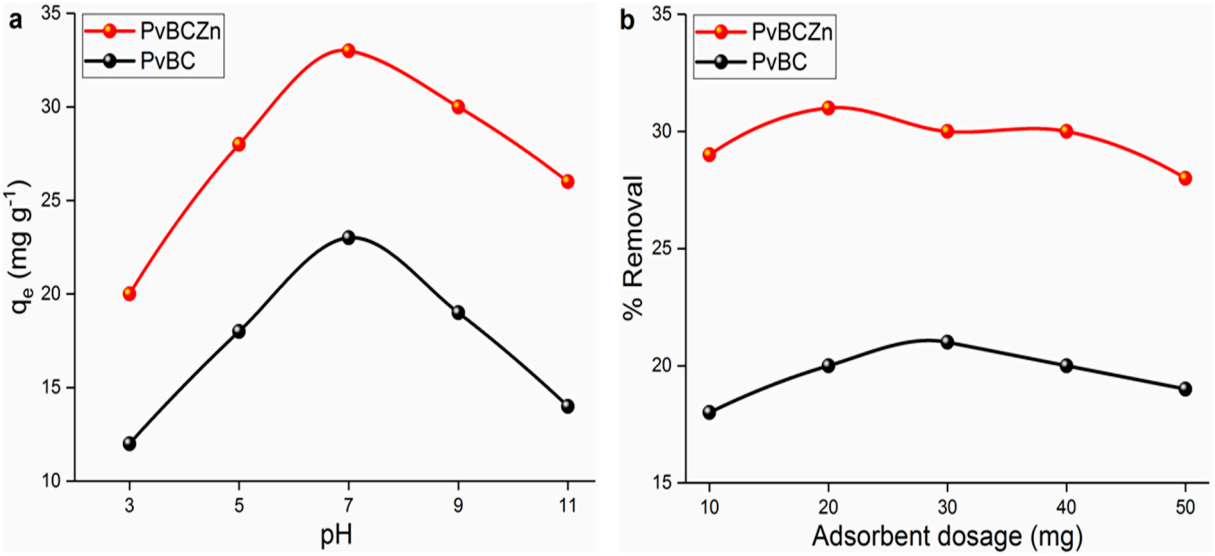

Figure 5. Effect of (**a**) pH and (**b**) adsorbent dosage on adsorption of primamycin la.

The best adsorbent for Primamycin la was found to be PvBCZn with the highest adsorption capacity of 34.51 mg/g at pH = 7.5 (Figure 5a). The maximum adsorption capacity increased to pH 7.0 and then decreased. This may be due to the repulsive forces between the drug and the adsorbent. The active ingredient of Primamycin la, oxytetracycline, has three acid dissociation constants (pKa) and four different forms depending on the pH of the solution [39]. The maximum adsorption capacity at pH 7.5 corresponds to the range where oxytetracycline passes into the neutral form. In the neutral form, weak electrostatic repulsion forces occur between drug molecules and PvBCZn, and the adsorption efficiency increases. After pH 7.5, with the transition of oxytetracycline into the anionic form, the electrostatic repulsion forces between the adsorbent surface and drug molecules increase, which leads to a decrease in the adsorption capacity.

As shown in Figure 5b, no significant increase and/or decrease in adsorption efficiency was observed in the adsorbent dosage. This slight change can be explained by the fact that as the adsorbent dosage increases, the probability of interaction between the empty active sites and drug molecules decreases and the adsorbent does not agglomerate at the amounts used.

3.8. Adsorption Isotherms and Kinetics

To understand the mechanism behind adsorption and the rate at which the pollutant is adsorbed on the surface, the adsorption reaction was carried out at different time intervals, and kinetic parameters were calculated using pseudo-first-order, pseudo-second-order and Elovich kinetic models (Table 3). For this purpose, 50 mL of milk solutions, including 20 mg/L of primamycin la, was taken, and the reaction was carried out at pH 7.5 using 25 mg of adsorbents (Figure 6a). The pseudo-first-order kinetic model is based on the assumption that adsorption is limited to active sites on the surface and is often used to estimate initial adsorption rates. The pseudo-second-order model emphasizes chemisorption and electron exchange or sharing at the adsorbent surface. The Elovich kinetic model is used to describe the process of chemisorption, especially on heterogeneous surfaces, and assumes that the adsorption rate is directly related to the unoccupied active sites on the surface.

Table 3. Kinetic model data of primamycin la adsorption on both PvBC and PvBCZn.

Kinetic Model	Parameters	PvBC	PvBCZn
Pseudo-first-order (PFO)	k_1 (min^{-1})	0.0761	0.1014
	q_e (mg/g)	24.0800	33.0164
	R^2	0.9619	0.9886
Pseudo-second-order (PSO)	k_2 (g/(mg.min))	0.0029	0.0035
	q_e (mg/g)	29.5872	37.8372
	R^2	0.9396	0.9911
Elovich	β (g/mg)	0.1460	0.1361
	α (mg/(g.min))	4.4492	14.2314
	R^2	0.9071	0.9311

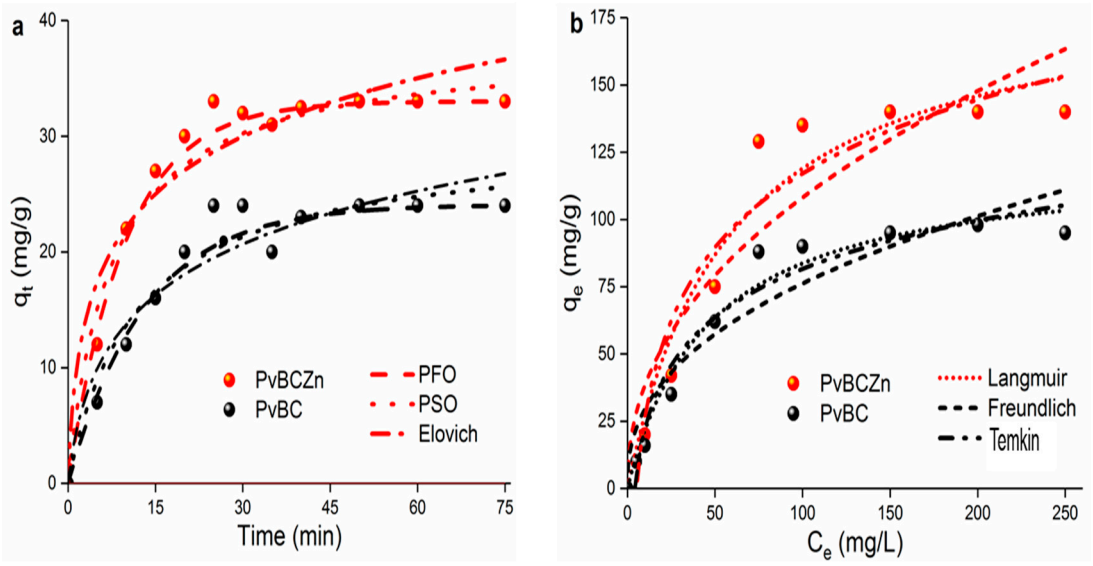

Figure 6. Adsorption (**a**) kinetics and (**b**) isotherms of primamycin la onto PvBC and PvBCZn adsorbents.

The Langmuir, Freundlich and Temkin isotherm models were used to describe the relationship between adsorbate and adsorbent at equilibrium temperature (Figure 6b). For this purpose, drug solutions of different concentrations (2–250 mg/L) were prepared and the adsorption process was carried out to evaluate the maximum adsorption capacity, and the data obtained are shown in Table 4. The Langmuir isotherm focuses on homogeneous and monolayer adsorption. One of the main features of the Langmuir isotherm is that

it can calculate the maximum capacity of adsorption (q_{max}) and the saturation state of the adsorbent surface. In addition, the Langmuir isotherm assumes that each adsorption point on the surface has equivalent energy. The Freundlich isotherm describes multilayer adsorption on heterogeneous surfaces, where the surface energy varies according to the adsorption points. The Temkin model assumes that the adsorption energy shows a linear decrease at low and high concentrations. From the R^2 values in Tables 3 and 4, it is seen that the adsorption of oxytetracycline by PvBCZn is in accordance with the Langmuir isotherm and pseudo-second-order kinetic model.

Table 4. Isotherm model data of primamycin la adsorption on both PvBC and PvBCZn.

Isotherm Model	Parameters	PvBC	PvBCZn
Langmuir	K_L (L/mg)	0.0216	0.0171
	q_m (mg/g)	122.4907	188.4817
	R^2	0.9710	0.9702
Freundlich	K_F (mg/g)/[(mg/L)^n]	11.5469	13.6514
	1/n	0.4098	0.4495
	R^2	0.8549	0.8582
Temkin	K_T (L/mg)	0.2360	0.1941
	B (J/mol)	25.8319	39.4940
	R^2	0.9551	0.9342

Assumptions for the possible adsorption mechanism are as follows:

(a) Oxytetracycline can create electrostatic attraction with Zn ions on the BC surface. Zinc ions are positively charged and can interact with the negative groups of oxytetracycline.

(b) Zn ions can be replaced with metallic ions or other cations on the BC surface. This can allow for the adsorption of oxytetracycline on the surface.

(c) The aromatic rings of oxytetracycline can perform the π-π stacking interactions with organic compounds on the BC surface.

Oxytetracycline removals from different environments with different adsorbents are compared in Table 5.

Table 5. Comparison of adsorbents used for oxytetracycline removal.

Adsorbent	Sample	Adsorbent Dosage (mg)	Contact Time (min)	Adsorption (mg/g)	Reference
PvBC	Milk	25	60	122.49	This work
PvBCZn	Milk	25	60	188.48	This work
PKC-4	Water	10	180	543	[40]
ZIF-8	Water	10	240	312	[41]
MIP1	Milk	20	15	96%	[6]
MIP2	Eggs/Honey	20	24 h	-	[42]

The stability and reusability of an adsorbent are very important in both economic and practical applications. To test the stability and reusability of PvBCZn, after adsorption, the adsorbent was desorbed in a water/alcohol mixture for 12 h. Then, it was pyrolyzed at 600 °C for 2 h and then used directly for the adsorption of oxytetracycline in milk samples. This process was repeated four times, and after five cycles, the adsorption capacity decreased by 8% (Figure 7); thus, it is concluded that PvBCZn has efficient stability and reusability.

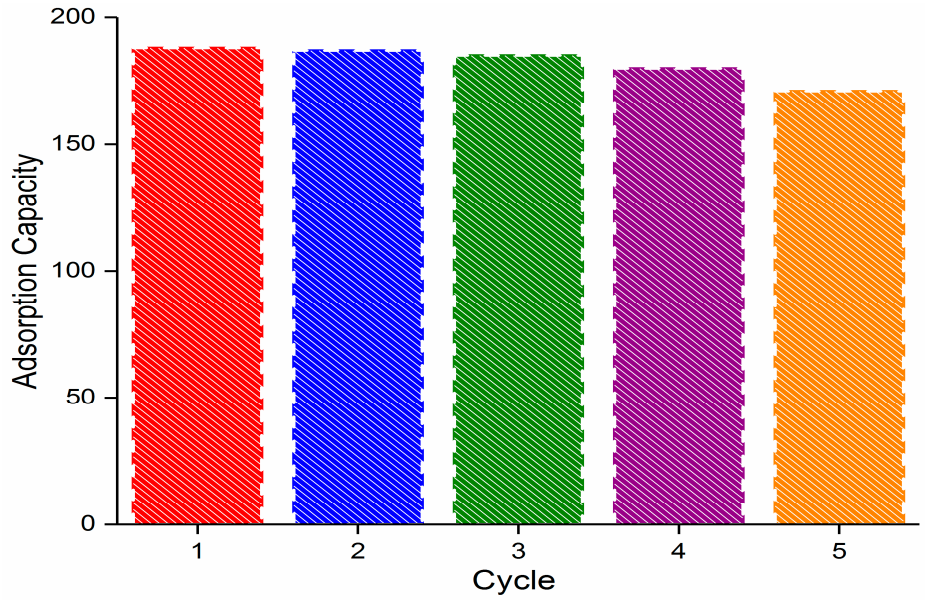

Figure 7. The impact of cycles on the adsorption capacity of PvBCZn for the removal of primamycin Ia from milk.

4. Conclusions

In this study, both PvBC obtained by the pyrolysis of bean plant and PvBCZn obtained by the activation of PvBC with $ZnCl_2$ were used as adsorbents for the removal of primamycin la from a milk sample. From the characterization results, PvBC was successfully activated. PvBCZn showed a higher adsorption capacity at the optimum conditions of pH and adsorbent dosage, which were found to be 7.5 and 25 mg, respectively. Based on the results of moisture content, water solubility, swelling behavior, antimicrobial activity and adsorption capacity, PvBCZn has the potential to be used as an adsorbent for the removal of primamycin la from a milk sample. Considering its reusability, it was concluded that it is an economical adsorbent since it has a stable structure. It was concluded that more effective biochar-activated adsorbents can be synthesized by conducting studies with different chemicals at different ratios and different pyrolysis temperatures.

Author Contributions: Conceptualization: M.Ş.; Data Curation: M.Ş. and C.R.L.-D.; Investigation: M.Ş. and C.R.L.-D.; Methodology: M.Ş., Y.A., C.R.L.-D., J.H.L.-D. and R.C.C.; Software: M.Ş., Y.A., J.H.L.-D. and R.C.C.; Writing—Original Draft: M.Ş., Y.A., J.H.L.-D. and R.C.C.; Reviewing: M.Ş., Y.A., C.R.L.-D., J.H.L.-D. and R.C.C. All authors have read and agreed to the published version of the manuscript.

Funding: This research received no external funding.

Data Availability Statement: The data that support the findings of this study are available from the corresponding author upon reasonable request.

Conflicts of Interest: All authors declare that there is not any commercial or associative interest that represents a conflict of interest in connection with the work submitted.

References

1. Girma, K.; Tilahun, Z.; Haimanot, D. Review on milk safety with emphasis on ıts public health. *World J. Dairy Food Sci.* **2014**, *9*, 166–183. [CrossRef]
2. Ruhí, A.; Acuña, V.; Barceló, D.; Huerta, B.; Mor, J.R.; Rodríguez-Mozaz, S.; Sabater, S. Bioaccumulation and trophic magnification of pharmaceuticals and endocrine disruptors in a Mediterranean river food web. *Sci. Total Environ.* **2016**, *540*, 250–259. [CrossRef]
3. Barbooti, M.M.; Su, H.; Punamiya, P.; Sarkar, D. Oxytetracycline sorption onto Iraqi montmorillonite. *Int. J. Environ. Sci. Technol.* **2014**, *11*, 69–76. [CrossRef]

4. Rakshit, S.; Sarkar, D.; Punamiya, P.; Datta, R. Kinetics of oxytetracycline sorption on magnetite nanoparticles. *Int. J. Environ. Sci. Technol.* **2014**, *11*, 1207–1214. [CrossRef]
5. Fu, B.; Ge, C.; Yue, L.; Luo, J.; Feng, D.; Deng, H.; Yu, H. Characterization of biochar derived from pineapple peel waste and its application for sorption of oxytetracycline from aqueous solution. *BioResources* **2016**, *11*, 9017–9035. [CrossRef]
6. Aguilar, J.F.F.; Miranda, J.M.; Rodriguez, J.A.; Paez-Hernandez, M.E.; Ibarra, I.S. Selective removal of tetracycline residue in milk samples using a molecularly imprinted polymer. *J. Polym. Res.* **2020**, *27*, 176. [CrossRef]
7. Abbood, N.S.; Ali, N.S.; Khader, E.H.; Majdi, H.S.; Albayati, T.M.; Saady, N.M.C. Photocatalytic degradation of cefotaxime pharmaceutical compounds onto a modified nanocatalyst. *Res. Chem. Intermed.* **2023**, *49*, 43–56. [CrossRef]
8. Ding, C.; Zhu, Q.; Yang, B.; Petropoulos, E.; Xue, L.; Feng, Y.; He, S.; Yang, L. Efficient photocatalysis of tetracycline hydrochloride (TC-HCl) from pharmaceutical wastewater using AgCl/ZnO/g-C_3N_4 composite under visible light: Process and mechanisms. *J. Environ. Sci.* **2023**, *126*, 249–262. [CrossRef]
9. Tripathy, P.; Prakash, O.; Sharma, A.; Panchal, D.; Pal, S. Chapter 7—Antibiotics in wastewater: Perspective of biological treatment processes. In *Degradation of Antibiotics and Antibiotic-Resistant Bacteria from Various Sources*; Academic Press: Cambridge, MA, USA, 2023; pp. 159–177. [CrossRef]
10. Alfonso-Muniozguren, P.; Serna-Galvis, E.A.; Bussemaker, M.; Torres-Palma, R.A.; Lee, J. A review on pharmaceuticals removal from waters by single and combined biological, membrane filtration and ultrasound systems. *Ultrason. Sonochem.* **2021**, *76*, 105656. [CrossRef]
11. Bosio, M.; Souza-Chaves, B.M.; Saggioro, E.M.; Bassin, J.P.; Dezotti, M.W.C.; Quinta-Ferreira, M.E.; Quinta-Ferreira, R.M. Electrochemical degradation of psychotropic pharmaceutical compounds from municipal wastewater and neurotoxicity evaluations. *Environ. Sci. Pollut. Res.* **2021**, *28*, 23958–23974. [CrossRef] [PubMed]
12. García-Espinoza, J.D.; Nacheva, P.M. Degradation of pharmaceutical compounds in water by oxygenated electrochemical oxidation: Parametric optimization, kinetic studies and toxicity assessment. *Sci. Total Environ.* **2019**, *691*, 417–429. [CrossRef] [PubMed]
13. Klatt, M.; Beyer, F.; Einfeldt, J. Hospital wastewater treatment and the role of membrane filtration—Removal of micropollutants and pathogens: A review. *Water Sci. Technol.* **2022**, *86*, 2213–2232. [CrossRef]
14. Nadour, M.; Boukraa, F.; Benaboura, A. Removal of Diclofenac, Paracetamol and Metronidazole using a carbon-polymeric membrane. *J. Environ. Chem. Eng.* **2019**, *7*, 103080. [CrossRef]
15. Camargo-Perea, A.L.; Serna-Galvis, E.A.; Lee, J.; Torres-Palma, R.A. Understanding the effects of mineral water matrix on degradation of several pharmaceuticals by ultrasound: Influence of chemical structure and concentration of the pollutants. *Ultrason. Sonochem.* **2021**, *73*, 105500. [CrossRef]
16. Ghanbari, F.; Hassani, A.; Wacławek, S.; Wang, Z.; Matyszczak, G.; Lin, K.Y.A.; Dolatabadi, M. Insights into paracetamol degradation in aqueous solutions by ultrasound-assisted heterogeneous electro-Fenton process: Key operating parameters, mineralization and toxicity assessment. *Sep. Purif. Technol.* **2021**, *266*, 118533. [CrossRef]
17. Ganiyu, S.O.; Oturan, N.; Raffy, S.; Cretin, M.; Causserand, C.; Oturan, M.A. Efficiency of plasma elaborated sub-stoichiometric titanium oxide (Ti_4O_7) ceramic electrode for advanced electrochemical degradation of paracetamol in different electrolyte media. *Sep. Purif. Technol.* **2019**, *208*, 142–152. [CrossRef]
18. Yun, W.C.; Lin, K.Y.A.; Tong, W.C.; Lin, Y.F.; Du, Y. Enhanced degradation of paracetamol in water using sulfate radical-based advanced oxidation processes catalyzed by 3-dimensional Co_3O_4 nanoflower. *Chem. Eng. J.* **2019**, *373*, 1329–1337. [CrossRef]
19. Şahin, M.; Arslan, Y. Adsorptive and oxidative removal of naproxen and diclofenac using Ag NPs, Cu NPs and Ag/Cu NPs. *Res. Chem. Intermed.* **2023**, *8*, 3627–3643. [CrossRef]
20. Şahin, M.; Arslan, Y.; Tomul, F. Removal of naproxen and diclofenac using magnetic nanoparticles/nanocomposites. *Res. Chem. Intermed.* **2022**, *48*, 5209–5226. [CrossRef]
21. Caicedo, D.F.; Reis, G.S.D.; Lima, E.C.; de Brum, I.A.S.; Thue, P.S.; Cazacliu, B.G.; Lima, D.R.; Santos, A.H.; Dotto, G.L. Efficient adsorbent based on construction and demolition wastes functionalized with 3-aminopropyltriethoxysilane (APTES) for the removal ciprofloxacin from hospital synthetic effluents. *J. Environ. Chem. Eng.* **2020**, *8*, 103875. [CrossRef]
22. Thue, P.S.; Umpierres, C.S.; Lima, E.C.; Lima, D.R.; Machado, F.M.; Reis, G.S.D.; da Silva, R.S.; Pavan, F.A.; Tran, H.N. Single-step pyrolysis for producing magnetic activated carbon from tucumã (*Astrocaryum aculeatum*) seed and nickel(II) chloride and zinc(II) chloride. Application for removal of nicotinamide and propanolol. *J. Hazard. Mater.* **2020**, *398*, 122903. [CrossRef]
23. Zhang, L.; Yao, L.; Ye, L.; Long, B.; Dai, Y.; Ding, Y. Benzimidazole-based hyper-cross-linked polymers for effective adsorption of chlortetracycline from aqueous solution. *J. Environ. Chem. Eng.* **2020**, *8*, 104562. [CrossRef]
24. Álvarez-Torrellas, S.; Rodríguez, A.; Ovejero, G.; García, J. Comparative adsorption performance of ibuprofen and tetracycline from aqueous solution by carbonaceous materials. *Chem. Eng. J.* **2016**, *283*, 936–947. [CrossRef]
25. Sewu, D.D.; Jung, H.; Kim, S.S.; Lee, D.S.; Woo, S.H. Decolorization of cationic and anionic dye-laden wastewater by steam-activated biochar produced at an industrial-scale from spent mushroom substrate. *Bioresour. Technol.* **2019**, *277*, 77–86. [CrossRef] [PubMed]

26. Boakye, P.; Lee, C.W.; Lee, W.M.; Woo, S.H. The Cell Viability on Kelp and Fir Biochar and the Effect on the Field Cultivation of Corn. *Clean Technol.* **2016**, *22*, 29–34. [CrossRef]
27. Chahinez, H.O.; Abdelkader, O.; Leila, Y.; Tran, H.N. One-stage preparation of palm petiole-derived biochar: Characterization and application for adsorption of crystal violet dye in water. *Environ. Technol. Innov.* **2020**, *19*, 100872. [CrossRef]
28. Tran, H.N.; Tomul, F.; Ha, N.T.H.; Nguyen, D.T.; Lima, E.C.; Le, G.T.; Chang, C.T.; Masindi, V.; Woo, S.H. Innovative spherical biochar for pharmaceutical removal from water: Insight into adsorption mechanism. *J. Hazard. Mater.* **2020**, *394*, 122255. [CrossRef]
29. Yunus, Z.M.; Al-Gheethi, A.; Othman, N.; Hamdan, R.; Ruslan, N.N. Removal of heavy metals from mining effluents in tile and electroplating industries using honeydew peel activated carbon: A microstructure and techno-economic analysis. *J. Clean. Prod.* **2020**, *251*, 119738. [CrossRef]
30. Leite, A.B.; Saucier, C.; Lima, E.C.; Reis, G.S.D.; Umpierres, C.S.; Mello, B.L.; Shirmardi, M.; Dias, S.L.P.; Sampaio, C.H. Activated carbons from avocado seed: Optimisation and application for removal of several emerging organic compounds. *Environ. Sci. Pollut. Res.* **2018**, *25*, 7647–7661. [CrossRef]
31. Tran, H.N.; Lee, C.K.; Vu, M.T.; Chao, H.P. Removal of Copper, Lead, Methylene Green 5, and Acid Red 1 by Saccharide-Derived Spherical Biochar Prepared at Low Calcination Temperatures: Adsorption Kinetics, Isotherms, and Thermodynamics. *Water Air Soil Pollut.* **2017**, *228*, 401. [CrossRef]
32. Nguyen, T.B.; Truong, Q.M.; Chen, C.W.; Doong, R.A.; Chen, W.H.; Dong, C.D. Mesoporous and adsorption behavior of algal biochar prepared via sequential hydrothermal carbonization and $ZnCl_2$ activation. *Bioresour. Technol.* **2022**, *346*, 126351. [CrossRef] [PubMed]
33. Tian, D.; Xu, Z.; Zhang, D.; Chen, W.; Cai, J.; Deng, H.; Sun, Z.; Zhou, Y. Micro-mesoporous carbon from cotton waste activated by $FeCl_3/ZnCl_2$: Preparation, optimization, characterization and adsorption of methylene blue and eriochrome black T. *J. Solid State Chem.* **2019**, *269*, 580–587. [CrossRef]
34. Brown, K.; Mugoh, M.; Call, D.R.; Omulo, S. Antibiotic residues and antibioticresistant bacteria detected in milk marketed for human consumption in Kibera, Nairobi. *PLoS ONE* **2020**, *15*, e0233413. [CrossRef] [PubMed]
35. Gülpınar, M.; Tomul, F.; Arslan, Y.; Tran, H.N. Chitosan-based film incorporated with silver-loaded organo-bentonite or organo-bentonite: Synthesis and characterization for potential food packaging material. *Int. J. Biol. Macromol.* **2024**, *274*, 133197. [CrossRef] [PubMed]
36. Naima, A.; Ammar, F.; Abdelkader, O.; Rachid, C.; Lynda, H.; Syafiuddin, A.; Boopathy, R. Development of a novel and efficient biochar produced from pepper stem for effective ibuprofen removal. *Bioresour. Technol.* **2022**, *347*, 126685. [CrossRef]
37. Li, Y.; Zimmerman, A.R.; He, F.; Chen, J.; Han, L.; Chen, H.; Hu, X.; Gao, B. Solvent-free synthesis of magnetic biochar and activated carbon through ball-mill extrusion with Fe_3O_4 nanoparticles for enhancing adsorption of methylene blue. *Sci. Total Environ.* **2020**, *722*, 137972. [CrossRef] [PubMed]
38. Yadav, S.; Asthana, A.; Singh, A.K.; Chakraborty, R.; Vidya, S.S.; Susan, M.A.B.H.; Carabineiro, S.A.C. Adsorption of cationic dyes, drugs and metal from aqueous solutions using a polymer composite of magnetic/β-cyclodextrin/activated charcoal/Na alginate: Isotherm, kinetics and regeneration studies. *J. Hazard. Mater.* **2021**, *409*, 124840. [CrossRef]
39. Lye, J.W.P.; Saman, N.; Sharuddin, S.S.N.; Othman, N.S.; Mohtar, S.S.; Noor, A.M.M.; Buhari, J.; Cheu, S.C.; Kong, H.; Mat, H. Removal Performance of Tetracycline and Oxytetracycline from Aqueous Solution via Natural Zeolites: An Equilibrium and Kinetic Study. *CLEAN Soil Air Water* **2017**, *45*, 1600260. [CrossRef]
40. Wei, Z.; Hou, C.; Gao, Z.; Wang, L.; Yang, C.; Li, Y.; Liu, K.; Sun, Y. Preparation of Biochar with Developed Mesoporous Structure from Poplar Leaf Activated by $KHCO_3$ and Its Efficient Adsorption of Oxytetracycline Hydrochloride. *Molecules* **2023**, *28*, 3188. [CrossRef] [PubMed]
41. Li, N.; Zhou, L.; Jin, X.; Owens, G.; Chen, Z. Simultaneous removal of tetracycline and oxytetracycline antibiotics from wastewater using a ZIF-8 metal organic-framework. *J. Hazard. Mater.* **2018**, *366*, 563–572. [CrossRef]
42. Kong, J.; Wang, Y.; Nie, C.; Ran, D.; Jia, X. Preparation of magnetic mixed-templates molecularly imprinted polymer for the separation of tetracycline antibiotics from egg and honey samples. *Anal. Methods* **2012**, *4*, 1005–1011. [CrossRef]